International Journal of Pediatric Otorhinolaryngology 159 (2022) 111204

Contents lists available at ScienceDirect

International Journal of Pediatric Otorhinolaryngology

journal homepage: www.elsevier.com/locate/ijporl

Cochlear base length as predictor for angular insertion depth in incomplete partition type 2 malformations

Wilhelm Wimmer [a,b,*], Fabio O. Soldati [b], Stefan Weder [a,b], Mattheus Vischer [b], Georgios Mantokoudis [a,b], Marco Caversaccio [a,b], Lukas Anschuetz [a,b]

[a] Hearing Research Laboratory, ARTORG Center for Biomedical Engineering Research, University of Bern, Switzerland
[b] Department of Otorhinolaryngology, Head & Neck Surgery, Inselspital, Bern University Hospital, University of Bern, 3008, Bern, Switzerland

ARTICLE INFO

Keywords:
Cochlear duct length
A-value
Insertion depth
Mondini dysplasia
Incomplete partition type 2

ABSTRACT

Introduction: The preoperative determination of suitable electrode array lengths for cochlear implantation in inner ear malformations is a matter of debate. The choice is usually based on individual experience and the use of intraoperative probe electrodes. The purpose of this case series was to evaluate the applicability and precision of an angular insertion depth (AID) prediction method, based on a single measurement of the cochlear base length (CBL).

Methods: We retrospectively measured the CBL in preoperative computed tomography (CT) images in 10 ears (8 patients) with incomplete partition type 2 malformation. With the known electrode length (linear insertion depth, LID) the AID at full insertion was retrospectively predicted for each ear with a heuristic equation derived from non-malformed cochleae. Using the intra- or post-implantation cone beam CT images, the actual AID was assessed and compared. The deviations of the predicted from the actual insertion angles were quantified (clinical prediction error) to assess the precision of this single-measure estimation.

Results: Electrode arrays with 15 mm (n = 3), 19 mm (n = 2), 24 mm (n = 3), and 26 mm (n = 2) length were implanted. Postoperative AIDs ranged from 211° to 625°. Clinical AID prediction errors from −64° to 62° were observed with a mean of 0° (SD of 44°). In two ears with partial insertion of the electrode, the predicted AID was overestimated. The probe electrode was intraoperatively used in 9/10 cases.

Conclusion: The analyzed method provides good predictions of the AID based on LID and CBL. It does not account for incomplete insertions, which lead to an overestimation of the AID. The probe electrode is useful and well established in clinical practice. The investigated method could be used for patient-specific electrode length selection in future patients.

1. Introduction

Congenital sensorineural hearing loss affects 2–4/1000 children [1,2], with up to 20–25% of the cases being associated with inner ear malformations, depending on the population [3,4]. According to the morphological classification of Sennaroglu & Saatci (2002), the incomplete partition type 2 (IP-2) describes a hypoplastic cochlea with 1.5 turns, in which the middle and apical turns coalesce to form a cystic apex [5,6]. It is associated with a dilated vestibule and enlarged vestibular aqueduct (EVA) [5,7]. The simultaneous presence of all three malformations is commonly referred to as "Mondini dysplasia" [5,7,8]. The responsible developmental arrest in the embryonic period is thought to be in the seventh week, resulting in osseous malformations [3,5] as well as immaturity of neuronal tissue [9,10].

Profound sensorineural hearing loss due to IP-2 malformations is an indication for a cochlear implant (CI) [6,11–13] with favorable outcomes comparable to children undergoing CI without inner ear malformations [14]. Precondition is the identification of the cochlear nerve in magnetic resonance tomography [15]. However, CI surgery can be challenging in cases of inner ear malformations due to possible

Abbreviations: AID, angular insertion depth; LID, linear insertion depth; CBL, cochlear base length; IP-2, incomplete partition type 2; EVA, enlarged vestibular aqueduct; CBCT, cone beam computed tomography.

* Corresponding author. Hearing Research Laboratory, ARTORG Center for Biomedical Engineering Research, University of Bern, Murtenstrasse 50, CH-3008, Bern, Switzerland.
E-mail address: wilhelm.wimmer@unibe.ch (W. Wimmer).

https://doi.org/10.1016/j.ijporl.2022.111204
Received 20 February 2022; Received in revised form 26 May 2022; Accepted 5 June 2022
Available online 9 June 2022

abnormal course of the facial nerve, endolymphatic gusher or morphological abnormalities that hinder optimal placement of the CI array [6,16]. Morphometric analyses demonstrated that malformed inner ears have a significantly smaller cochlear base length (CBL) and width, and also smaller tilt angles between the first and second turn compared to non-malformed inner ears [17,18].

The clinical applicability of a preoperative estimation of appropriate electrode array lengths for specific insertion depths are currently intensely investigated [8,11,18,19]. The insertion depth of an electrode array is characterized as angular insertion depth (AID, in degrees) or linear insertion depth (LID, in mm). In malformed inner ears, the electrode array choice is usually based on surgical experience and the intraoperative use of probe electrodes. Only few recommendations are found based on neuroradiological imaging. For IP-2 malformations, Flex 24 or Form 24 are proposed to achieve one full turn without taking the CBL into account [8,11]. Based on high-resolution CT, an actual AID of maximum 450–540° was suggested [18,19].

In the presented case series, we aimed to apply a single-measure method for estimating AIDs in malformed cochleae [20]. We hypothesized that the existing equation, which showed beneficial clinical applicability [19] for non-malformed cochleae, could be applied to estimate the AID in malformed cochleae and facilitate the electrode array choice in pediatric cases with IP-2.

2. Patients and methods

2.1. Study design and data collection

We performed a retrospective cross-sectional study including all children with IP-2 malformation who received a CI between 2013 and 2021. Formal ethical approval was not required by the local institutional review board for this kind of case series. The study was performed according to the declaration of Helsinki.

We analyzed pre- and intra- or postoperative computed-tomography (CT) and cone beam computed-tomography (CBCT) scans. Cases with missing pre- or postoperative imaging were excluded. Epidemiologic data on age and sex, as well as the medical history and context, were extracted from the medical records. Surgical reports provided information about surgical approach, use of probe electrode and decision of the electrode array and the insertion success (full/partial insertion based on surgeon's assessment and intra- or postoperative imaging). Audiologic reports included data from the intraoperative neural response telemetry, impedances, number of postoperatively activated electrodes, speech understanding, and user satisfaction. The following paragraphs explain the applied method. The equation was originally presented and validated in a Thiel-fixed temporal bone study [20]. Its usefulness and clinical applicability in normal cochleae was confirmed in a study by Rathgeb et al. [19].

2.2. Preoperative angular insertion depth prediction

To measure the dimensions of the basal turn, the cochlea needs to be correctly visualized [20]. We retrospectively measured the cochlear base length (CBL) in preoperative CT (Siemens SOMATOM, slice thickness: 0.4 mm, field of view: 80 mm, voxel size: 0.156 × 0.156 × 0.200 mm^3, effective dose ~2.0 mSv) images using our clinical PACS system (SECTRA IDS7, Linköping, Sweden). For visualization, we aligned an oblique slice through the basal turn that is orthogonal to the modiolar axis [21]. An example of the measurement is illustrated in Fig. 1a. After assessment of the CBL, the following heuristic equation was used to estimate the angular insertion depth (AID) in degrees for a defined electrode array length (LID) in mm and CBL in mm [20]:

$$\mathrm{AID} = 248 \cdot \left(e^{\mathrm{LID}/(2.43 \cdot \mathrm{CBL})} - 1\right)$$

For lateral wall electrode array insertion depth estimation, a free interactive calculator is available online (www.artorg.unibe.ch/research/hrl/data/ci_insertion_depth_estimator). The equation estimates the radiological position of the center of the most apical electrode. As the silicone tip of the electrode array is not visible in the radiograph, the LID needs to be corrected depending on the electrode array type. For example, in the case presented in Fig. 1, an electrode array with 15 mm length and an approximately 0.5 mm long silicone tip (Compressed array, MED-EL) was used. Therefore, the corrected LID value is 14.5 mm (15–0.5 mm). With a CBL of 8.2 mm this results in a predicted AID of:

$$248 \cdot \left(e^{14.5/(2.43 \cdot 8.2)} - 1\right) = 265°$$

Other free-fitting electrode array types have different silicone tip lengths, which should be taken into account for the estimation (e.g., ~1 mm for MED-EL Flex series and ~0.5 mm for Form[19], Compressed, or Medium arrays; ~0.5 mm for Advance Bionics HiFocus 1j® arrays; ~0.5 mm for Cochlear Slim Straight® arrays; ~1 mm for Oticon Medical Evo® arrays).

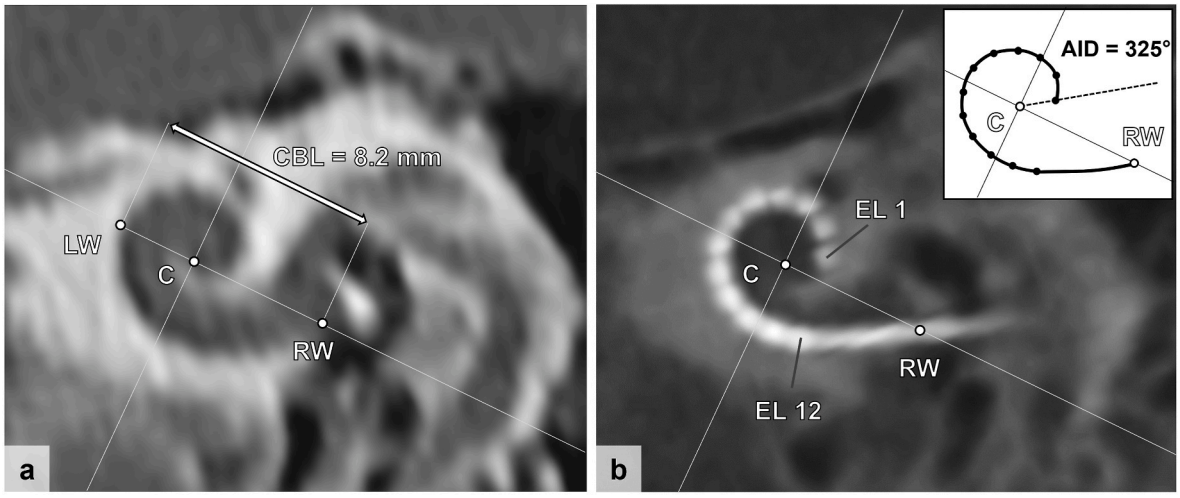

Fig. 1. Radiological assessment of the cochlear base length (CBL) and angular insertion depth (AID) using multiplanar reconstruction. **a)** In the preoperative image, the basal turn is visualized and the round window (RW), the center of the modiolus in the basal turn (C), and the lateral wall intersection (LW) are identified. The cochlear base length (CBL) is measured between the RW and LW landmarks. **b)** Postoperative visualization of the basal turn with inserted electrode array (15 mm length, corrected 14.5 mm, MED-EL Compressed). The AID is measured between the zero-degree reference line passing through the RW and the most apical electrode (EL1).

2.3. Ground truth for angular insertion depth and clinical prediction error

We assessed the AID ground truth, i.e., the achieved insertion depth in intra- or postoperative CBCT (Xoran XCAT, slice thickness: 0.3 mm, field of view: 140 mm, voxel size: 0.3 × 0.3 × 0.3 mm^3, effective dose ~0.4 mSv) images using our clinical PACS system (SECTRA IDS7, Linköping, Sweden). The center of the round window and the center of the modiolus in the basal turn were identified to define the zero degree reference line [19,22]. The AID was then measured from the zero degree reference line to the center of the most apical electrode as illustrated in Fig. 1b [19].

We calculated the clinical prediction error as the difference between the predicted AID (using the preoperative images and equation) and the actual postoperative AID (postoperative ground truth) [19]. For the example presented in Fig. 1, the clinical prediction error was 265–325 = −60°, indicating an underestimation of the electrode array insertion depth.

3. Results

In our institution, nine children with IP-2 malformation were unilaterally or bilaterally implanted with a CI between 2013 and 2021. In all cases, MED-EL (Innsbruck, Austria) implants were used. Preoperative (CT) and intra- or postoperative (CBCT) images of 8 children (6 right ears, 4 left ears) were analyzed for this study. One child did not receive postoperative imaging and was excluded. A summary of all cases is presented in Table 1. The mean age at implantation was 5 years and 4 months, ranging from 10 months to 8 years and 8 months. The contralateral ear was in 2 cases a combined cochlea and cochlear nerve aplasia, in 6 cases also an IP-2 malformation, in one case hearing loss of unknown cause. Only one child had a normal contralateral ear and hearing.

3.1. Angular insertion depth and clinical prediction error

Pre- and postoperative radiograph-based AID outcomes are summarized in Table 2. Overall, postoperative AIDs from 211° to 625° were observed. The average CBL was 8.5 mm (standard deviation 0.4 mm). The clinical AID prediction error ranged from −64° (underestimation) to 62° (overestimation). The average clinical prediction error was 0° (standard deviation of 44°). For partial CI array insertions (2 cases), the predicted AID was always overestimated (i.e., positive clinical prediction error). Two cases of full insertions were inserted beyond the silicon stopper of the electrode array.

Table 1
Overview of investigated cases with IP-2 malformation.

Case	Sex	Side	Age at implantation	Medical history/context
1	Female	Right	1.0 y	Cochlear and cochlear nerve aplasia left
2	Female	Right	8.3 y	Constitutional growth delay
3*	Female	Left	6.6 y	Otogenic meningitis after otitis media (right) with labyrinthitis and mastoiditis, bilateral vestibulopathy, neurological deficiencies, panel for genetic hearing loss non-conclusive
4*	Female	Right	6.7 y	See case 3
5	Female	Right	8.3 y	Mild contusion capitis followed by hearing loss and perilymphatic fistula
6**	Female	Right	2.9 y	No other pathologies
7**	Female	Left	7.6 y	No other pathologies
8	Male	Left	0.8 y	Cochlear and cochlear nerve aplasia right
9	Female	Right	8.7 y	USH2A missense-mutation. Patent ductus arteriosus, cerebral palsy, psychomotor development delay, optic atrophy
10	Male	Left	2.9 y	Unclear syndromal disease, vesicoureteric reflux, speech-delay

*,** Cases of bilateral implantation in the same subjects.

3.2. Surgical and functional outcomes

The surgical and functional implantation outcomes are presented in Table 3. In 9 of 10 cases the use of a probe electrode before CI array insertion was reported. Among these, in five cases, a smooth insertion of the probe electrode was possible. In the remaining four cases, the surgeons encountered resistance and decided to choose shorter electrode arrays. Neural response telemetry showed large variability in outcomes ranging from no responses at all to normal responses with all electrodes. Interestingly, the responses were not consistent with the functional outcomes. Word recognition scores in the German Freiburg monosyllabic word list ranged from 25 to 85%. Testing was not yet performed in 3 cases and the postoperative interval for testing was not homogeneous in the other cases.

4. Discussion

In the presented case series of IP-2 malformations, we analyzed the applicability of a single-measure method based on CBL for AID prediction. Postoperative AIDs (211°–625°) and clinical AID prediction errors (−64°–62°) were observed with a mean clinical prediction error of 0°. The probe electrode was used in 9/10 cases and encountered resistance in 4 cases. As already suggested by another applicability study we found the method overestimates the AID due to the occurrence of unexpected partial insertions [19]. Partial insertions were expected as cochlear implantation in inner ear malformations lead to more incomplete insertions than in normal cochleae [6].

Overall, the used heuristic equation provided useful predictions of the AID for a given LID and CBL [20]. For IP-2 malformations, Flex24 or Form24 are generally proposed to achieve one full turn without taking the CBL into account [8,11]. The hereby evaluated estimation method may be a step toward patient-specific electrode array selection [18,23,24]. A patient specific recommended LID (resp. electrode length) could be calculated based on a target AID and the CBL (Fig. 2).

However, no target AID for IP-2 malformation has been described yet. Based on high-resolution CT, an actual AID of maximum 450–540° was suggested [18,19]. Interestingly, our results show AIDs of more than 540 up to even 625° (1.7 turns), which were inserted without resistance. However, 540° AID should not be used as target, since it may be underestimated, and the electrode consecutively inserted too deep. In this context, potential complications are the rupture of the basilar membrane, other internal structures or the dislocation into the scala vestibuli [25–27]. On the other hand, it is desirable to maximize cochlear coverage to potentially improve neural tissue stimulation and thus outcome [28,29]. IP-2 malformations have fewer ganglion cells in the first 1.5 turns [9,30]. A histopathological study showed that radiological-pathological correlation can even be inconsistent. They reported an IP-2 malformation, where internal structures were found in the basal, middle and even apical turn [31]. However, the above-mentioned complications associated with insertion-trauma may limit such deep insertions. Our results revealed an underestimation of the AID of 60° and 64° degrees in two cases. Since an AID of 540° is considered to be the maximum, a target AID of up to 450° can be considered safe [18].

In the future, a prospective evaluation of the LID prediction (electrode length) based on the measurement of the CBL would be an interesting topic. A tentative proposed AID target range for cochlear implantation in IP-2 malformations of e.g. one full turn up to 450° should be evaluated [8,11,18,19]. An overview of proposed electrode array lengths for different angular insertion depths and cochlear base lengths is provided in Fig. 2. This suggestion can be considered as a rule of thumb for a basic clinical application and needs to be refined, depending on the cochlear anatomy e.g., the number of available turns.

Table 2
Radiological outcomes: Preoperative prediction and postoperative angular insertion depth (AID).

Case	Inserted Electrode array	Full array length (mm)	Corrected array length (mm)	CBL (mm)	Predicted AID (°)	Actual AID (°)	Clinical prediction error (°)	Inserted electrodes
1	Form 19	19	18.5	8.1	387	378	9	Full (12/12)
2	Flex 24	24	23.0	8.7	488	440	48	Full (12/12)
3*	Compressed	15	14.5	8.2	265	325	−60	Full (12/12)[a]
4*	Compressed	15	14.5	8.3	261	230	31	Partial (11/12)
5	Flex 24	24	23.0	8.4	517	524	−7	Full (12/12)
6**	Compressed	15	14.5	8.8	241	211	30	Full (12/12)
7**	Flex 24	24	23.0	8.9	470	408	62	Partial (10/12)
8	Flex 26	26	25.0	9.2	511	550	−39	Full (12/12)
9	Form 19	19	18.5	8.1	387	393	−6	Full (12/12)
10	Flex 26	26	25.0	8.7	561	625	−64	Full (12/12)[a]

*,** Cases of bilateral implantation in the same subjects.
[a] Cases of over inserted electrode arrays.

Table 3
Summary of surgical and functional implantation outcomes.

Case	Surgical approach	Notable details	Intraoperative use of probe electrode	ECAP responses	Activated electrodes	User satisfaction
1	RW	Gusher	Used, no array change	1 to 11	12/12	Very good
2	RW		Used, no array change	1 to 12	12/12	Initially good, later non-user
3*	CO	Scar tissue in the cochlea	Used, switched to compressed	2 and 9	12/12	Very good
4*	RW		Used, switched to compressed	No responses	12/12	Very good
5	RW		Used, no array change	1 to 11	12/12	Very good
6**	RW	Gusher	Used, switched to compressed	1 to 12	12/12	Very good
7**	RW	Gusher	Unknown	1 to 10	10/12	Very good
8	RW		Used, no array change	1 to 12	12/12	Unknown
9	RW		Used, switched to Form19	1 to 12	12/12	Recent implantation
10	RW		Used, no array change	1 to 12	12/12	Recent implantation

*,** Cases of bilateral implantation in the same subjects.

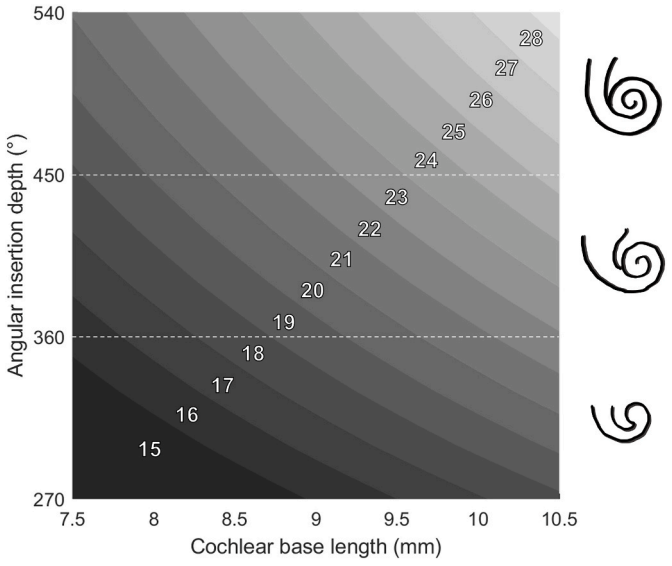

Fig. 2. Electrode array lengths in millimeters depending on cochlear base length and targeted angular insertion depth. Electrode array lengths were estimated using the heuristic equation reported in Anschuetz et al. [20]. The array lengths indicate the radiologically visible electrode contacts and do not include the invisible silicone tip.

Nowadays, an intraoperative probe electrode can be used to determine the most suitable electrode length. However, the probe electrode may cause itself a trauma to the endocochlear membranous structures. Ideally, the presented prediction method could possibly replace the probe electrode in the future and allow insertion with less trauma.

Only in one case, a reduced number of electrodes were activated postoperatively (10/12 electrodes). Of all inner ear malformations, the group of incomplete partitions was reported to have the same number of activated electrodes postoperatively as control patients (10.5 vs 10.25 electrodes, 12 potential electrodes) [10]. All inner ear malformations together have significantly fewer activated electrodes on average (8.25 electrodes) [10]. We expected a wide variability in neural response telemetry, since the otic epithelium during the embryonic phase and the number of ganglion cells are reduced and the exact distribution of neural tissue is not entirely known [9,10]. In our case series, gusher occurred in 3 out of 10 cases. In IP-2 cases with enlarged vestibular aqueduct (n = 197), gusher occurs in 48.6% of all cases without impact on speech perception or language outcomes [14].

IP-2 malformations may be missed in newborn hearing screening, since they manifest from severe hearing loss to normal hearing at young age [7,8]. Therefore, regular hearing checks in pediatric routine screening to detect progression and early intervention are of major importance [32]. Case 4 showed progressive hearing loss after mild head trauma which has been suggested to be a progression factor [7]. Since a short duration of profound deafness is one of the most important positive predictor of audiological outcome and speech perception, a favorable result was possible even at a relatively old age (Case 4: 8.3 y) [33,34].

With the viewer we used, the interobserver variability is considered low [19]. Different imaging modalities (i.e., preoperative CT vs. post-operative CBCT) were used in the process. In the case of congenital malformations in children, our standard protocol involves the use of CBCT imaging, because it provides reduced radiation while enabling to detect electrode contacts with sufficient accuracy [19,25].

4.1. Limitations

Our study is limited by its retrospective nature and the small number of included ears. Not the precision of electrode lengths prediction, rather the precision of an AID prediction method was analyzed. The method cannot predict the occurrence of incomplete insertions. Electrode arrays from a single manufacturer were analyzed, which reduces the strength

of the study. In an overview of cochlear implant electrode array designs, other manufacturers and the key features of cochlear implants are described [24]. The method is based on the measurement of a single value (CBL), which is defined in cochleae with normal anatomy and is significantly smaller in inner ear malformations [17,18]. The CBL does not capture the full complexity of inner ear morphology [16]. Moreover, the prediction method relies on the identification of anatomical landmarks resulting in inter- and intra-rater variability and introducing additional estimation errors [35,36].

5. Conclusion

The analyzed method is able to provide good predictions of the AID based on LID and CBL. It does not account for incomplete insertions, which lead to an overestimation of the AID. To use the method for preoperative selection of the electrode array length, a target AID needs to be defined.

Funding

This research did not receive any specific grant from funding agencies in the public, commercial or not-for-profit sectors.

Declaration of competing interest

No conflict of interest to declare. LA is consultant for Stryker ENT.

Acknowledgements

none.

References

[1] K.R. White, Early hearing detection and intervention programs: opportunities for genetic services, Am. J. Med. Genet. 130A (2004) 29–36, https://doi.org/10.1002/ajmg.a.30048.
[2] R.J.H. Smith, J.F. Bale, K.R. White, Sensorineural hearing loss in children, Lancet 365 (2005) 879–890, https://doi.org/10.1016/S0140-6736(05)71047-3.
[3] R.K. Jackler, W.M. Luxford, W.F. House, Congenital malformations of the inner ear: a classification based on embryogenesis, Laryngoscope 97 (1987) 2–14, https://doi.org/10.1002/lary.5540971301.
[4] E.A. van Beeck Calkoen, M.S.D. Engel, J.M. van de Kamp, H.G. Yntema, S. T. Goverts, M.F. Mulder, P. Merkus, E.F. Hensen, The etiological evaluation of sensorineural hearing loss in children, Eur. J. Pediatr. 178 (2019) 1195–1205, https://doi.org/10.1007/s00431-019-03379-8.
[5] L. Sennaroglu, I. Saatci, A new classification for cochleovestibular malformations, Laryngoscope 112 (2002) 2230–2241, https://doi.org/10.1097/00005537-200212000-00019.
[6] Z. Farhood, S.A. Nguyen, S.C. Miller, M.A. Holcomb, T.A. Meyer, H.G. Rizk, Cochlear implantation in inner ear malformations: systematic review of speech perception outcomes and intraoperative findings, Otolaryngol. Head Neck Surg. 156 (2017) 783–793, https://doi.org/10.1177/0194599817696502.
[7] L. Sennaroglu, M. Demir Bajin, Classification of inner ear malformations, in: K. Kaga (Ed.), Cochlear Implantation in Children with Inner Ear Malformation and Cochlear Nerve Deficiency, Springer, 2016.
[8] L. Sennaroğlu, M.D. Bajin, Classification and current management of inner ear malformations, Balkan Med. J. 34 (2017) 397–411, https://doi.org/10.4274/balkanmedj.2017.0367.
[9] J.M. Schmidt, Cochlear neuronal populations in developmental defects of the inner ear. Implications for cochlear implantation, Acta Otolaryngol. 99 (1985) 14–20, https://doi.org/10.3109/00016488509119140.
[10] M. Sainz, J. Garcia-Valdecasas, E. Fernandez, M.T. Pascual, O. Roda, Auditory maturity and hearing performance in inner ear malformations: a histological and electrical stimulation approach, Eur. Arch. Oto-Rhino-Laryngol. 269 (2012) 1583–1587, https://doi.org/10.1007/s00405-011-1792-7.
[11] N. Schwartz, K.D. Brown, L.R. Park, Audiologic outcomes of cochlear implantation in cochlear malformations: a comparative analysis of lateral wall and perimodiolar electrode arrays, Otol. Neurotol. 41 (2020), e1201, https://doi.org/10.1097/MAO.0000000000002833. –e1206.
[12] L.-S. Kim, S.-W. Jeong, M.-J. Huh, Y.-D. Park, Cochlear implantation in children with inner ear malformations, Ann. Otol. Rhinol. Laryngol. 115 (2006) 205–214, https://doi.org/10.1177/000348940611500309.
[13] M.N. Pakdaman, B.S. Herrmann, H.D. Curtin, J. Van Beek-King, D.J. Lee, Cochlear implantation in children with anomalous cochleovestibular anatomy: a systematic review, Otolaryngol. Head Neck Surg. 146 (2012) 180–190, https://doi.org/10.1177/0194599811429244.
[14] L. Benchetrit, N. Jabbour, S. Appachi, Y.-C. Liu, M.S. Cohen, S. Anne, Cochlear implantation in pediatric patients with enlarged vestibular aqueduct: a systematic review, Laryngoscope (2021), https://doi.org/10.1002/lary.29742.
[15] H.B. Ozkan, B. Cicek Cinar, E. Yucel, G. Sennaroglu, L. Sennaroglu, Audiological performance in children with inner ear malformations before and after cochlear implantation: a cohort study of 274 patients, Clin. Otolaryngol. 46 (2021) 154–160, https://doi.org/10.1111/coa.13625.
[16] A. Dhanasingh, Variations in the size and shape of human cochlear malformation types, Anat. Rec. 302 (2019) 1792–1799, https://doi.org/10.1002/ar.24136.
[17] R. Martinez-Monedero, J.K. Niparko, N. Aygun, Cochlear coiling pattern and orientation differences in cochlear implant candidates, Otol. Neurotol. 32 (2011) 1086–1093, https://doi.org/10.1097/MAO.0b013e31822a1ee2.
[18] T. Khurayzi, F. Almuhawas, A. Alsanosi, Y. Abdelsamad, Ú. Doyle, A. Dhanasingh, A novel cochlear measurement that predicts inner-ear malformation, Sci. Rep. 11 (2021) 7339, https://doi.org/10.1038/s41598-021-86741-x.
[19] C. Rathgeb, M. Demattè, A. Yacoub, L. Anschuetz, F. Wagner, G. Mantokoudis, M. Caversaccio, W. Wimmer, Clinical applicability of a preoperative angular insertion depth prediction method for cochlear implantation, Otol. Neurotol. 40 (2019) 1011–1017, https://doi.org/10.1097/MAO.0000000000002304.
[20] L. Anschuetz, S. Weder, G. Mantokoudis, M. Kompis, M. Caversaccio, W. Wimmer, Cochlear implant insertion depth prediction: a temporal bone accuracy study, Otol. Neurotol. 39 (2018), e996, https://doi.org/10.1097/MAO.0000000000002034 e1001.
[21] B.M. Verbist, M.W. Skinner, L.T. Cohen, P.A. Leake, C. James, C. Boëx, T. A. Holden, C.C. Finley, P.S. Roland, J.T. Roland, M. Haller, J.F. Patrick, C.N. Jolly, M.A. Faltys, J.J. Briaire, J.H.M. Frijns, Consensus panel on a cochlear coordinate system applicable in histologic, physiologic, and radiologic studies of the human cochlea, Otol. Neurotol. 31 (2010) 722–730, https://doi.org/10.1097/MAO.0b013e3181d279e0.
[22] W. Wimmer, F. Venail, T. Williamson, M. Akkari, N. Gerber, S. Weber, M. Caversaccio, A. Uziel, B. Bell, Semiautomatic cochleostomy target and insertion trajectory planning for minimally invasive cochlear implantation, BioMed Res. Int. 2014 (2014), 596498, https://doi.org/10.1155/2014/596498.
[23] S. Manolidis, R. Tonini, J. Spitzer, Endoscopically guided placement of prefabricated cochlear implant electrodes in a common cavity malformation, Int. J. Pediatr. Otorhinolaryngol. 70 (2006) 591–596, https://doi.org/10.1016/j.ijporl.2005.07.004.
[24] A. Dhanasingh, C. Jolly, An overview of cochlear implant electrode array designs, Hear. Res. 356 (2017) 93–103, https://doi.org/10.1016/j.heares.2017.10.005.
[25] W. Wimmer, B. Bell, M.E. Huth, C. Weisstanner, N. Gerber, M. Kompis, S. Weber, M. Caversaccio, Cone beam and micro-computed tomography validation of manual array insertion for minimally invasive cochlear implantation, Audiol. Neuro. Otol. 19 (2014) 22–30, https://doi.org/10.1159/000356165.
[26] M.B. Fitzgerald, W.H. Shapiro, P.D. McDonald, H.S. Neuburger, S. Ashburn-Reed, S. Immerman, D. Jethanamest, J.T. Roland, M.A. Svirsky, The effect of perimodiolar placement on speech perception and frequency discrimination by cochlear implant users, Acta Otolaryngol. 127 (2007) 378–383, https://doi.org/10.1080/00016480701258671.
[27] A.A. Eshraghi, N.W. Yang, T.J. Balkany, Comparative study of cochlear damage with three perimodiolar electrode designs, Laryngoscope 113 (2003) 415–419, https://doi.org/10.1097/00005537-200303000-00005.
[28] B.P. O'Connell, A. Cakir, J.B. Hunter, D.O. Francis, J.H. Noble, R.F. Labadie, G. Zuniga, B.M. Dawant, A. Rivas, G.B. Wanna, Electrode location and angular insertion depth are predictors of audiologic outcomes in cochlear implantation, Otol. Neurotol. 37 (2016) 1016–1023, https://doi.org/10.1097/MAO.0000000000001125.
[29] B.P. O'Connell, J.B. Hunter, D.S. Haynes, J.T. Holder, M.M. Dedmon, J.H. Noble, B. M. Dawant, G.B. Wanna, Insertion depth impacts speech perception and hearing preservation for lateral wall electrodes, Laryngoscope 127 (2017) 2352–2357, https://doi.org/10.1002/lary.26467.
[30] W.H. Slattery, W.M. Luxford, Cochlear implantation in the congenital malformed cochlea, Laryngoscope 105 (1995) 1184–1187, https://doi.org/10.1288/00005537-199511000-00008.
[31] K.J. Leung, A.M. Quesnel, A.F. Juliano, H.D. Curtin, Correlation of CT, MR, and histopathology in incomplete partition-II cochlear anomaly, Otol. Neurotol. 37 (2016) 434–437, https://doi.org/10.1097/MAO.0000000000001027.
[32] M.L. Bush, B. McNulty, J.B. Shinn, Does adherence to early infant hearing detection and intervention guidelines positively impact pediatric speech outcomes? Laryngoscope 131 (2021) 1693–1694, https://doi.org/10.1002/lary.28994.
[33] S.-W. Jeong, L.-S. Kim, A new classification of cochleovestibular malformations and implications for predicting speech perception ability after cochlear implantation, Audiol. Neuro. Otol. 20 (2015) 90–101, https://doi.org/10.1159/000365584.
[34] N. Bernhard, U. Gauger, E. Romo Ventura, F.C. Uecker, H. Olze, S. Knopke, T. Hänsel, A. Coordes, Duration of deafness impacts auditory performance after cochlear implantation: a meta-analysis, Laryngoscope Investig. Otolaryngol. 6 (2021) 291–301, https://doi.org/10.1002/lio2.528.
[35] J.E. Iyaniwura, M. Elfarnawany, S. Riyahi-Alam, M. Sharma, Z. Kassam, Y. Bureau, L.S. Parnes, H.M. Ladak, S.K. Agrawal, Intra- and interobserver variability of cochlear length measurements in clinical CT, Otol. Neurotol. 38 (2017) 828–832, https://doi.org/10.1097/MAO.0000000000001411.
[36] W. Wimmer, C. Vandersteen, N. Guevara, M. Caversaccio, H. Delingette, Robust cochlear modiolar Axis detection in CT, Med. Image Comput. Comput. Assist. Interv. 22 (2019) 3–10, https://doi.org/10.1007/978-3-030-32254-0_1.